High-efficiency organic electrophosphorescent devices with tris(2-phenylpyridine)iridium doped into electron-transporting materials

Adachi, Chihaya
Center for Photonics and Optoelectronic Materials (POEM), Department of Electrical Engineering and the Princeton Materials Institute, Princeton University

Baldo, Marc.A.
Center for Photonics and Optoelectronic Materials (POEM), Department of Electrical Engineering and the Princeton Materials Institute, Princeton University

Forrest, Stephen R.
Center for Photonics and Optoelectronic Materials (POEM), Department of Electrical Engineering and the Princeton Materials Institute, Princeton University

Thompson, Mark E.
Department of Chemistry, University of Southern California

出版情報：Applied Physics Letters. 77 (6), pp.904-906, 2000-08-07. American Institute of Physics
バージョン：

High-efficiency organic electrophosphorescent devices with tris(2-phenylpyridine)iridium doped into electron-transporting materials

Chihaya Adachi, Marc A. Baldo, and Stephen R. Forrest
Center for Photonics and Optoelectronic Materials (POEM), Department of Electrical Engineering, Princeton University, Princeton, New Jersey 08544

Mark E. Thompson
Department of Chemistry, University of Southern California, Los Angeles, California 90089

(Received 19 April 2000; accepted for publication 7 June 2000)

We demonstrate high-efficiency organic light-emitting devices employing the green electrophosphorescent molecule, *fac* tris(2-phenylpyridine)iridium [$Ir(ppy)_3$], doped into various electron-transport layer (ETL) hosts. Using 3-phenyl-4-(1′-naphthyl)-5-phenyl-1,2,4-triazole as the host, a maximum external quantum efficiency (η_{ext}) of $15.4\pm0.2\%$ and a luminous power efficiency of 40 ± 2 lm/W are achieved. We show that very high internal quantum efficiencies (approaching 100%) are achieved for organic phosphors with low photoluminescence efficiencies due to fundamental differences in the relationship between electroluminescence from triplet and singlet excitons. Based on the performance characteristics of single and double heterostructures, we conclude that exciton formation in $Ir(ppy)_3$ occurs within close proximity to the hole-transport layer/ETL:$Ir(ppy)_3$ interface. © *2000 American Institute of Physics.* [S0003-6951(00)00332-6]

The recent demonstration[1,2] of high-efficiency organic light-emitting devices (OLEDs) using the electrophosphorescent molecules 2,3,7,8,12,13,17,18-octaethyl-21*H*,23*H*-porphine platinum (PtOEP) and *fac* tris(2-phenylpyridine) iridium ($Ir(ppy)_3$) led to the prospect of obtaining devices with internal quantum efficiencies (η_{int}) of 100% through radiative recombination of both singlet and triplet excitons. In previous studies,[2,3] an external quantum efficiency (η_{ext}) of 8% (corresponding to $\eta_{int}\sim40\%$) using a light-emitting layer (EML) comprised of $Ir(ppy)_3$ doped into a 4,4′-*N*,*N*′-dicarbazole-biphenyl (CBP) host was reported. This remarkable result was ascribed[4] to bipolar carrier transport in CBP along with a favorable triplet energy level alignment between the host and the dopant which promotes efficient energy transfer between species. In this study, we describe high-efficiency electrophosphorescent OLEDs employing an electron-transport layer (ETL) as a host. The ETL materials are 2,9-dimethyl-4,7-diphenyl-phenanthroline (BCP),[5] 1,3-bis(*N*,*N*-*t*-butyl-phenyl)-1,3,4-oxadiazole (OXD7),[6] and 3-phenyl-4-(1′-naphthyl)-5-phenyl-1,2,4-triazole (TAZ).[7] It has been previously established that these materials possess good electron-transport characteristics while also serving to block hole and exciton transport.[5–7] Our experiments are consistent with η_{int} approaching 100%, suggesting that future work on increasing efficiency will realize the largest gains by focusing on improving light out-coupling from the OLED structure.

Organic layers were deposited by high-vacuum (10^{-6} Torr) thermal evaporation onto a clean glass substrate precoated with an indium–tin–oxide (ITO) layer with a sheet resistance of ~20 Ω/□. A 60-nm-thick film of 4,4′-bis[*N*,*N*′-(3-tolyl)amino]-3,3′-dimethylbiphenyl[8] (HMTPD) served as the hole-transport layer (HTL). Next, a 25-nm-thick EML consisting of 6%–8% $Ir(ppy)_3$ was doped into various electron-transporting hosts via thermal codeposition. A 50-nm-thick layer of tris-(8-hydroxyquinoline)aluminum (Alq_3) was used to transport and inject electrons into the EML. A shadow mask with 1-mm-diam openings was used to define the cathode consisting of a 150-nm-thick Mg–Ag layer, with a 20-nm-thick Ag cap. Alternatively, the cathode consisted of a 100-nm-thick layer of Al–0.56 wt % Li.

Current density (J) versus voltage (V) measurements were obtained using a semiconductor parameter analyzer, with the luminance obtained by placing the OLEDs directly onto the surface of a large-area calibrated silicon photodiode, thus avoiding corrections needed to account for non-Lambertian spatial emission patterns.[3] The photoluminescence (PL) and electroluminescence (EL) transient decays were characterized using a streak camera following excitation by a nitrogen laser at a wavelength of $\lambda=337$ nm and a pulse width of ~500 ps for PL, and by a pulse generator for EL.

A maximum $\eta_{ext}=15.4\pm0.2\%$ and power efficiency of 40 ± 2 lm/W of the 7%-$Ir(ppy)_3$-doped TAZ device using an Al–Li cathode was obtained (see Fig. 1), corresponding to $\eta_{int}\cong80\%$. The value of η_{ext} is almost double compared with that previously reported for $Ir(ppy)_3$ devices[2] with η_{int} now approaching 100%. The device exhibits a gradual decrease in quantum efficiency with increasing current, characteristic of triplet–triplet annihilation observed in all electrophosphorescent devices.[11] Nevertheless, a high optical output power of 2.5 mW/cm^2 (corresponding to a luminance of ~4000 cd/m^2) with $\eta_{ext}=10.0\%$ was maintained even at $J=10$ mA/cm^2. At $Ir(ppy)_3$ concentrations less than 2%, we observed a decrease to $\eta_{ext}\sim3\%$ along with additional blue host emission ($\lambda\sim440$ nm), while at high $Ir(ppy)_3$ concentrations, a significant decrease in η_{ext} was also observed due to aggregate-induced quenching.

We summarize the performance of $Ir(ppy)_3$-doped OLEDs with four hosts and cathode metals, including previously reported data for CBP as a host[2] in the inset of Fig. 1. The use of an Al–Li cathode in TAZ-based devices slightly enhances η_{ext}, reflecting the improved electron-injection efficiency of Li over that of Mg due to the comparatively low work function of Li. We observed that both TAZ and OXD7

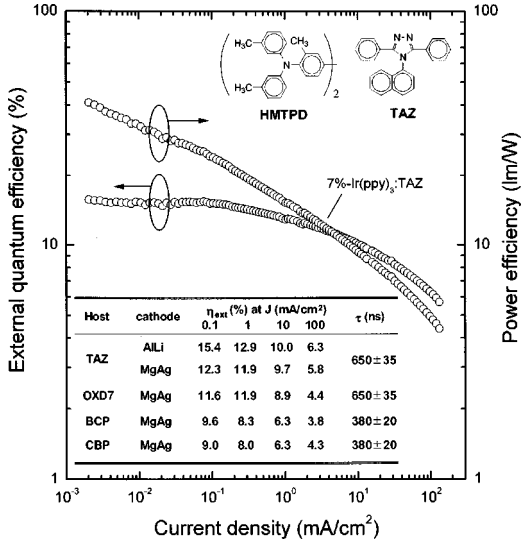

Host	cathode	η_{ext} (%) at J (mA/cm²) 0.1	1	10	100	τ (ns)
TAZ	AlLi	15.4	12.9	10.0	6.3	650±35
	MgAg	12.3	11.9	9.7	5.8	
OXD7	MgAg	11.6	11.9	8.9	4.4	650±35
BCP	MgAg	9.6	8.3	6.3	3.8	380±20
CBP	MgAg	9.0	8.0	6.3	4.3	380±20

FIG. 1. External quantum and power efficiencies of an ITO/HMTPD(60 nm)/7%-lr(ppy)$_3$:TAZ(25 nm)/Alq$_3$(50 nm)/Al–Li(100 nm) OLED. A maximum external quantum efficiency $\eta=15.4\%$ and power efficiency of 40 lm/W were obtained. **Insets**: The chemical structures of HMTPD and TAZ. External quantum efficiencies (η_{ext}) and photoluminescence decay times (τ) for lr(ppy)$_3$ doped into various hosts.

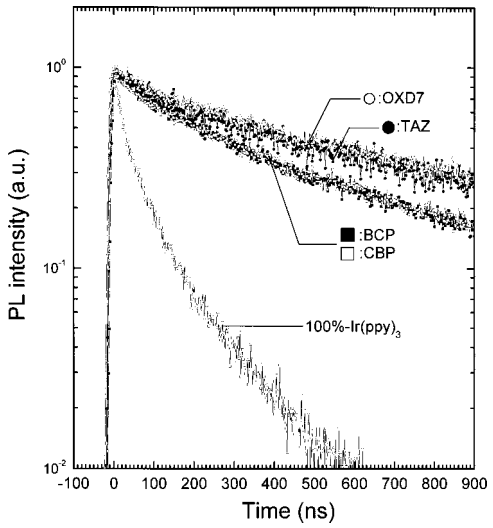

FIG. 2. Photoluminescence decay transients of 7%-lr(ppy)$_3$:OXD7(50 nm), 7%-lr(ppy)$_3$:TAZ(50 nm), 7%-lr(ppy)$_3$:BCP(50 nm), 7%-lr(ppy)$_3$:CBP(50 nm), and 100%-lr(ppy)$_3$(50 nm). Excitation power density is $\sim 5\times10^{16}$ cm^3.

showed comparably high values of η_{ext}, while devices with BCP and CBP hosts exhibited ~30% lower efficiencies. As shown Fig. 2, the room-temperature transient phosphorescent lifetime of 7%-Ir(ppy)$_3$:BCP in TAZ and OXD7 is $\tau=650\pm35$ ns, compared with $\tau=380\pm20$ ns in 7%-Ir(ppy)$_3$:BCP and 7%-Ir(ppy)$_3$:CBP. Since the phosphorescence efficiency is approximately proportional to the lifetime,[9] the longer lifetime in TAZ and OXD7 is consistent with the higher EL efficiencies of these devices. We note that all of the Ir(ppy)$_3$-doped hosts showed one order of magnitude longer lifetime compared to that of a neat film in which Ir(ppy)$_3$–Ir(ppy)$_3$ exciton interactions, i.e., ''self-quenching,'' increase the probability for nonradiative decay.

To elucidate the emission mechanisms leading to high efficiency, we varied the EML thickness from 2.5 to 30 nm while maintaining both the HTL and ETL thicknesses at 50 and 40 nm, respectively. This device is a single heterostructure (SH) due to the barrier to charge carriers and excitons only at the HTL/EML interface. These devices were compared with a double heterostructure[10] (DH) comprised of an EML sandwiched between the HTL (HMTPD) and a 10-nm-thick neat ETL, as shown in the inset of Fig. 3. Figure 3 shows the thickness dependence of η_{ext} at a fixed current density of 0.1 mA/cm^2 for both SH and DH devices using BCP as a host. At an EML thickness of <15 nm, a significant decrease of η_{ext} was observed in the SH device, while $\eta_{ext}=9\%$ was retained even with a 2.5-nm-thick EML in the DH device. This suggests the confinement of both charge carriers and triplet excitons within the very thin EML, characteristic of the DH architecture.

In both the SH and DH devices, the EL spectral shapes due to Ir(ppy)$_3$ triplet emission (with a peak wavelength of $\lambda_{max}=515$ nm) are independent of the EML thickness. Even in the SH structure with a 2.5-nm-thick EML, the spectral shape is identical to that of the neat Ir(ppy)$_3$ PL spectrum, with a negligible contribution from Alq$_3$.

The EL transient decays of the three devices are shown in Fig. 4. The DH device with a 2.5-nm-thick EML (curve i) shows an EL transient decay time ($\tau=320\pm15$ ns) comparable with that of the SH device ($\tau=380\pm20$ ns) with a 30-nm-thick EML (curve ii). The slightly reduced lifetime of the DH device may be due to a high density of triplet excitons confined within a very narrow EML, leading to enhanced triplet–triplet annihilation.[11] On the other hand, the SH device with a 2.5-nm-thick EML (curve iii) shows a very short lifetime ($\tau=50\pm3$ ns), suggesting the presence of significant dissipative nonradiative transitions. We note, also, that in the thinnest EML SH structure, the Ir(ppy)$_3$ triplets are strongly quenched by the adjacent Alq$_3$ layer with its significantly less energetic, nonradiative triplet state. The DH structure consisting of HMTPD and BCP double blocking

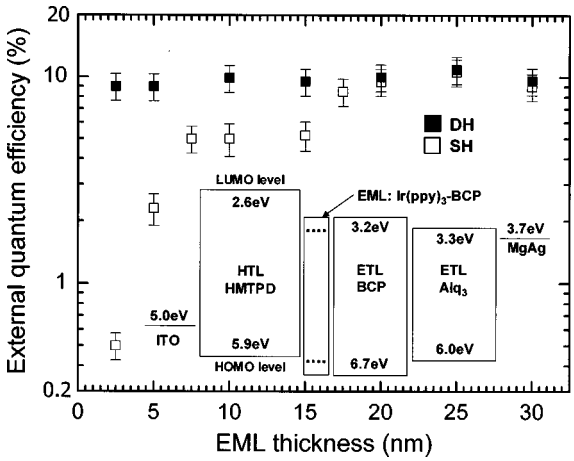

FIG. 3. External quantum efficiency (η) of single (SH) and double heterostructure (DH) OLEDs as a function of light-emitting-layer thickness. The SH and DH structures are composed of ITO/HMTPD(50 nm)/7%-lr(ppy)$_3$:BCP(variable)/Alq(40 nm)/MgAg(150 nm)/Ag(20 nm) and ITO/HMTPD(50 nm)/7%-lr(ppy)$_3$:BCP(variable)/BCP(10 nm)/Alq(40 nm)/MgAg(150 nm)/Ag(20 nm), respectively. In the DH structure, a high η was retained even with a light-emitting-layer thickness of only 2.5 nm. **Inset**: Energy levels of the constituent materials used in a DH OLED as referenced to vacuum. The highest occupied molecular orbital (HOMO) and the lowest unoccupied molecular orbital (LUMO) energies are indicated (see Ref. 19), and are unknown for lr(ppy)$_3$ (dashed lines).

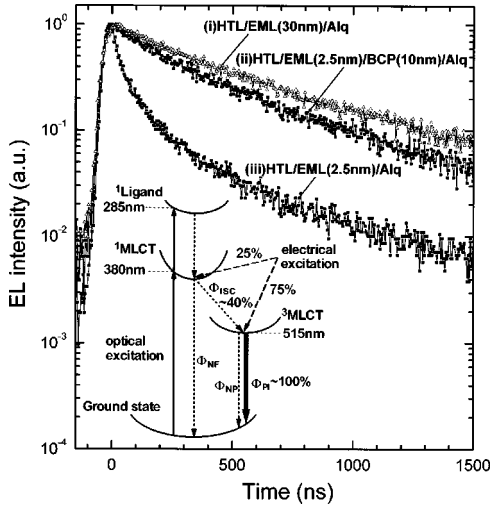

FIG. 4. Transient electroluminescence decay of the following: (i) single heterostructure (SH): ITO/HMTPD(50 nm)/7%-lr(ppy)$_3$:BCP(30 nm)/Alq(40 nm)/MgAg(150 nm)/Ag(20 nm), (ii) double heterostructure (DH): ITO/HMTPD(50 nm)/7%-lr(ppy)$_3$:BCP(2.5 nm)/BCP(10 nm)/Alq(40 nm)/MgAg(150 nm)/Ag(20 nm), and (iii) SH: ITO/HMTPD(50 nm)/7%-lr(ppy)$_3$:BCP(2.5 nm)/Alq(40 nm)/MgAg(150 nm)/Ag(20 nm) under a 100 ns, 9V pulse excitation. **Inset**: Energy-level diagram of lr(ppy)$_3$. The ligand singlet state (^{1}Ligand) and metal-to-ligand charge-transfer singlet state (^{1}MLCT) were determined by the absorption peaks in toluene solution (10^{-5} M). Also, the triplet MLCT state (^{3}MLCT) was estimated from the phosphorescence peak. Φ_{NF}, Φ_{ISC}, Φ_{PI}, and Φ_{NP} are quantum yields for nonemissive transitions from ^{1}MLCT, intersystem crossing, intrinsic phosphorescent transitions, and nonemissive transitions from ^{3}MLCT, respectively.

layers, in contrast, confines both charge carriers and triplet excitons even within a 2.5-nm-thick EML. The lack of blue fluorescence from either HMTPD or BCP suggests that leakage of electrons or holes into these adjacent layers is negligible. Finally, the time-resolved EL spectrum of this latter device is similar to neat Ir(ppy)$_3$, even during the initial ~20 ns after excitation. This, too, indicates that exciton formation occurs entirely within the EML, with little or no carrier recombination in the adjacent Alq$_3$ layer.

Two possible mechanisms lead to light emission: direct charge trapping by Ir(ppy)$_3$ or energy transfer from BCP to Ir(ppy)$_3$ followed by carrier recombination by BCP. Since BCP serves as both an electron-transporting and hole-blocking material,[5] holes can be directly injected from the HTL into the Ir(ppy)$_3$ highest occupied molecular orbital and trapped, where subsequently they combine with electrons which are transported across the BCP layer leading to direct exciton formation on Ir(ppy)$_3$. Alternatively, exciton formation may occur first on BCP, and then are subsequently transferred to Ir(ppy)$_3$ through Förster or Dexter processes, leading to efficient Ir(ppy)$_3$ emission. We are unable to determine which process is dominant since both occur within close proximity to the HTL/EML interface.

Finally, we discuss strategies for further improvement of EL efficiency of Ir(ppy)$_3$-doped devices. The inset of Fig. 4 shows the energy levels of an Ir(ppy)$_3$ molecule based on its absorption and emission spectra. We demonstrated here an internal efficiency of 80% by assuming that 20% of the emitted light is extracted from the structure.[12] However, the PL efficiency of Ir(ppy)$_3$ in a dilute solution is only 40% $\pm$10%.[13] In photoexcitation, phosphorescence takes place via intersystem crossing (ISC) from the metal-to-ligand charge-transfer singlet state (^{1}MLCT), since direct excitation to the triplet state (^{3}MLCT) is prohibited. Thus, the phosphorescence quantum yield (Φ_P) follows:

$$\Phi_P = \Phi_{\mathrm{ISC}} \frac{\kappa_P}{\kappa_P + \kappa_{\mathrm{NP}}}, \tag{1}$$

where Φ_{ISC} represents the probability for ISC, κ_P is the phosphorescence emission rate, and κ_{NP} that of nonemissive triplet decay. Under electrical excitation, both singlet and triplet excitons are directly created on either the guest or host molecules with a statistical splitting of $\chi \sim 25\%$ singlets and $(1-\chi) \sim 75\%$ triplets.[14] Thus, η_{int} follows:

$$\eta_{\mathrm{int}} = [(1-\chi) + \chi \Phi_{\mathrm{ISC}}] \frac{\kappa_P}{\kappa_P + \kappa_{\mathrm{NP}}}. \tag{2}$$

For consistent interpretation of both the EL and PL data, we conclude for Ir(ppy)$_3$ that $\kappa_P \gg \kappa_{\mathrm{NP}}$ and $\Phi_{\mathrm{ISC}} \cong 40\%$. Since the intrinsic phosphorescence efficiency $[\kappa_P/(\kappa_P+\kappa_{\mathrm{NP}})]$ is already near to its maximum value, further efficiency enhancement is limited even if we have $\Phi_{\mathrm{ISC}} = 100\%$. Hence, to further increase OLED efficiency beyond that obtained via electrophosphorescence, we must focus on schemes to increase light out-coupling by incorporating microcavities,[15] shaped substrates,[12,16] or an index-matching medium.[17,18] Also, phosphorescent materials with low-PL efficiencies appear to be useful in EL devices provided that the intrinsic phosphorescence efficiency is high.

The authors thank the Universal Display Corporation and the Defense Advanced Research Projects Agency for their support of this research. The authors thank M. Ohta at Ricoh Co. Ltd. for providing the hole-transport material.

[1] M. A. Baldo, D. F. O'Brien, Y. You, A. Shoustikov, S. Sibley, M. E. Thompson, and S. R. Forrest, Nature (London) **395**, 151 (1998).
[2] M. A. Baldo, S. Lamansky, P. E. Burrows, M. E. Thompson, and S. R. Forrest, Appl. Phys. Lett. **75**, 4 (1999).
[3] T. Tsutsui, M.-J. Yang, M. Yahiro, K. Nakamura, T. Watanabe, T. Tsuji, Y. Fukuda, T. Wakimoto, and S. Miyaguchi, Jpn. J. Appl. Phys., Part 2 **38**, L1502 (1999).
[4] H. Kanai, S. Ichinosawa, and Y. Sato, Synth. Met. **91**, 195 (1997).
[5] H. Nakada, S. Kawami, K. Nagayama, Y. Yonemoto, R. Murayama, J. Funaki, T. Wakimoto, and K. Imai, Polym. Prepr. Jpn., **35**, 2450 (1994).
[6] Y. Hamada, C. Adachi, T. Tsutsui, and S. Saito, Jpn. J. Appl. Phys., Part 1 **31**, 1812 (1992).
[7] J. Kido, K. Hongawa, K. Okuyama, and K. Nagai, Jpn. J. Appl. Phys., Part 2 **32**, L917 (1993).
[8] C. Adachi, K. Nagai, and N. Tamoto, Appl. Phys. Lett. **66**, 2679 (1995).
[9] M. Klessinger and J. Michl, *Excited States and Photochemistry of Organic Molecules* (VCH, New York, 1995).
[10] C. Adachi, T. Tsutsui, and S. Saito, Appl. Phys. Lett. **57**, 531 (1990).
[11] M. A. Baldo, C. Adachi, and S. R. Forrest (unpublished).
[12] G. Gu, D. Z. Garbuzov, P. E. Burrows, S. Venkatesh, and S. R. Forrest, Opt. Lett. **22**, 396 (1997).
[13] K. A. King, P. J. Spellane, and R. J. Watts, J. Am. Chem. Soc. **107**, 1431 (1985).
[14] W. Helfrich and W. G. Schneider, J. Chem. Phys. **44**, 2902 (1966).
[15] V. Bulovic, V. V. Khalfin, G. Gu, P. E. Burrows, D. Z. Garbuzov, and S. R. Forrest, Phys. Rev. B **58**, 3730 (1998).
[16] C. F. Madigan, M.-H. Lu, and J. C. Sturm, Appl. Phys. Lett. **76**, 1650 (2000).
[17] M. Borodilsky, T. F. Kraus, R. Coccioli, R. Vrijen, R. Bhat, and E. Yablonovitch, Appl. Phys. Lett. **75**, 1036 (1999).
[18] T. Yamazaki, K. Sumioka, and T. Tsutsui, Appl. Phys. Lett. **76**, 1243 (2000).
[19] I. G. Hill and A. Kahn, J. Appl. Phys. **85**, 6589 (1999).